

# Effects of pressure on the local atomic structure of $\text{CaWO}_4$ and $\text{YLiF}_4$ : mechanism of the scheelite-to-wolframite and scheelite-to-fergusonite transitions

D. Errandonea,<sup>a,b</sup> F.J. Manjón,<sup>c,\*</sup> M. Somayazulu,<sup>b</sup> and D. Häusermann<sup>b</sup>

<sup>a</sup>Departamento de Física Aplicada-ICMUV, Universitat de València, Edificio de Investigación, c/Dr. Moliner 50, 46100 Burjassot (Valencia), Spain

<sup>b</sup>HPCAT, Carnegie Institution of Washington, Advanced Photon Source, Building 434E, Argonne National Laboratory, 9700 South Cass Ave., Argonne, IL 60439, USA

<sup>c</sup>Departamento de Física Aplicada, Universitat Politècnica de València, Pl. Ferrandiz i Carbonell 2, 03801 Alcoy (Alicante), Spain

Received 21 July 2003; received in revised form 3 October 2003; accepted 24 October 2003

## Abstract

The pressure response of the scheelite phase of  $\text{CaWO}_4$  ( $\text{YLiF}_4$ ) and the occurrence of the pressure-induced scheelite-to-wolframite (M-fergusonite) transition are reviewed and discussed. It is shown that the change of the axial parameters under compression is related to the different pressure dependences of the W–O (Li–F) and Ca–O (Y–F) interatomic bonds. Phase transition mechanisms for both compounds are proposed. Furthermore, a systematic study of the phase transition in 16 different scheelite  $\text{ABX}_4$  compounds indicates that the transition pressure increases as the packing ratio of the anionic  $\text{BX}_4$  units around the  $A$  cations increases.

© 2003 Elsevier Inc. All rights reserved.

PACS: 61.10.Nz; 61.50.Ks; 62.50.+p

Keywords: Oxides; Fluorides; High pressure; X-ray diffraction; Phase transitions

## 1. Introduction

Many  $\text{ABX}_4$  compounds, like calcium tungstate ( $\text{CaWO}_4$ ) and yttrium lithium fluoride ( $\text{YLiF}_4$ ), crystallize in the tetragonal scheelite structure (SG:  $I4_1/a$ , No. 88,  $Z = 4$ ) [1,2] under ambient conditions. The strong interest in the structural stability of scheelite compounds under compression is evident in the numerous experimental studies on the pressure effects on their phase behavior [3–14]. In particular, it has been demonstrated recently that  $\text{CaWO}_4$  transforms under compression from the scheelite structure to the monoclinic wolframite structure (SG:  $P2/c$ , No. 13,  $Z = 2$ ) [1,2] at  $11 \pm 1$  GPa [3,4]. On the other hand,  $\text{YLiF}_4$  transforms under compression from the scheelite structure to the monoclinic M-fergusonite structure (SG:  $C2/c$ , No. 15,  $Z = 4$ ) [1,2] also at  $11 \pm 1$  GPa [5,6]. In both these compounds, the reversibility to the initial

scheelite structure after a decrease in the pressure has been shown.

From the cationic point of view, the scheelite structure consists of two intercalated diamond lattices: one for  $A$  cations and another for  $B$  cations (see Fig. 1), where the  $A$ – $A$  distances are equal to  $B$ – $B$  distances. In the scheelite structure,  $A$  cations, calcium (Ca) and yttrium (Y), are coordinated by eight  $X$  anions, oxygen (O) or fluorine (F), thus forming  $\text{AX}_8$  polyhedral units. On the other hand,  $B$  cations, tungsten (W) and lithium (Li), are coordinated by four  $X$  anions forming relatively isolated  $\text{BX}_4$  tetrahedral units [7]. In the cation coordination notation for  $\text{ABX}_4$  compounds ([cation  $A$  coordination–cation  $B$  coordination]), scheelites have cation coordination [8–4]. Fig. 1 shows a detail of the scheelite structure with the  $\text{AX}_8$  and  $\text{BX}_4$  polyhedra.

The study of the pressure effects on the local atomic structure can be a powerful tool for understanding the transformation mechanisms of the pressure-driven transitions. While a systematic analysis of the effects

\*Corresponding author. Fax: +34-96-652-84-09.

E-mail address: [fjmanjon@fis.upv.es](mailto:fjmanjon@fis.upv.es) (F.J. Manjón).

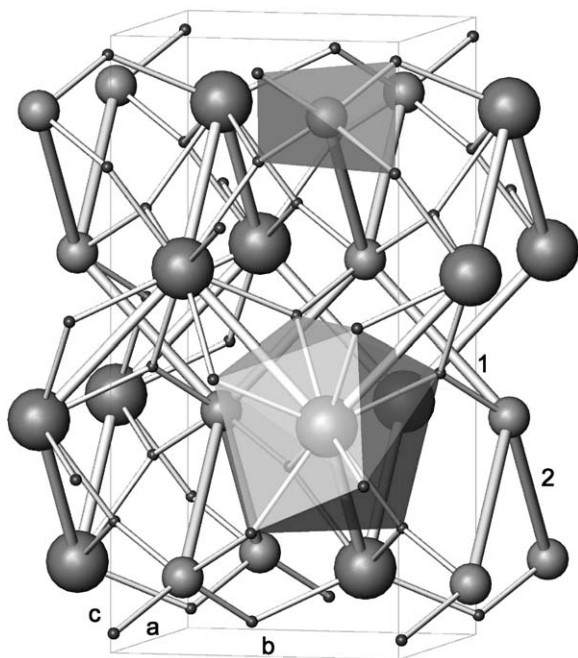


Fig. 1. Unit cell of the scheelite structure of  $ABX_4$  compounds with the  $a$ -,  $b$ - and  $c$ -axis. Big atoms refer to  $A$  cation (Ca, Y), the medium-sized atoms correspond to  $B$  cations (W, Li) and the small atoms to the  $X$  anion (O, F). Numbers 1 and 2 correspond to  $B$ - $B$  distances of the diamond-like structure along  $b+c$  and  $a+c$  directions, respectively. The  $AX_8$  polyhedra and the  $BX_4$  tetrahedra are shown.

of pressure on the local atomic structure of  $YLiF_4$  has already been performed [5], the same analysis in  $CaWO_4$  has not been performed yet. In this work, we report and discuss the pressure response of the local structure of W (Li) ions in  $CaWO_4$  ( $YLiF_4$ ) in the light of the recently reported high-pressure X-ray diffraction data [3,5] and other high-pressure techniques. The aim of discussing the effects of pressure in the local structure of both the compounds is to understand more precisely the occurrence of the scheelite-to-monoclinic transitions, and particularly, the scheelite-to-wolframite and scheelite-to-fergusonite transitions. From the characterization of the similarities and differences of the pressure response of the local structure of  $CaWO_4$  and  $YLiF_4$ , possible transformation mechanisms for both transitions are identified.

## 2. Experimental background

The lattice parameters and bond distances presented here for  $CaWO_4$  were obtained from the energy-dispersive X-ray powder diffraction (EDXD) patterns measured at the X-17C beamline at the National Synchrotron Light Source (NSLS) using a diamond-anvil-cell (DAC) at a diffraction angle  $2\theta = 13^\circ$ . As  $CaWO_4$  is soft (bulk modulus,  $B_0 = 77$  [3]), this material was used as its own quasi-hydrostatic pressure medium.

A detailed description of these experiments was given in Ref. [3]. There, we reported the occurrence of the scheelite-to-wolframite transition of  $CaWO_4$  at 11 GPa and its amorphization at 40 GPa, but we did not discuss the pressure effects on the local structure of the scheelite phase of  $CaWO_4$ . In the present paper, we report a detailed analysis of this issue, by comparing the pressure response of the local structure of  $CaWO_4$  and  $YLiF_4$ , in order to understand better the pressure behavior of the structure in the scheelite-type  $ABX_4$  compounds. In Fig. 2, we have shown an X-ray diffraction pattern of  $CaWO_4$  measured at 2 GPa. The spectrum is plotted together with the differences between the measured data and the calculated profile with the aim of illustrating the quality of the structural refinements used to extract the lattice parameters and bond lengths of  $CaWO_4$  presented here. In order to obtain the lattice parameters from the experimental data the Le Bail extraction technique [15] available in the GSAS programme [16] was employed. For every analyzed pressure, we obtained good agreement between the refined profiles and the experimental diffraction patterns, as illustrated in Fig. 2, and a low value for the residual for the intensities,  $R(F) < 0.15$  (for 52 reflections). The bond distances for

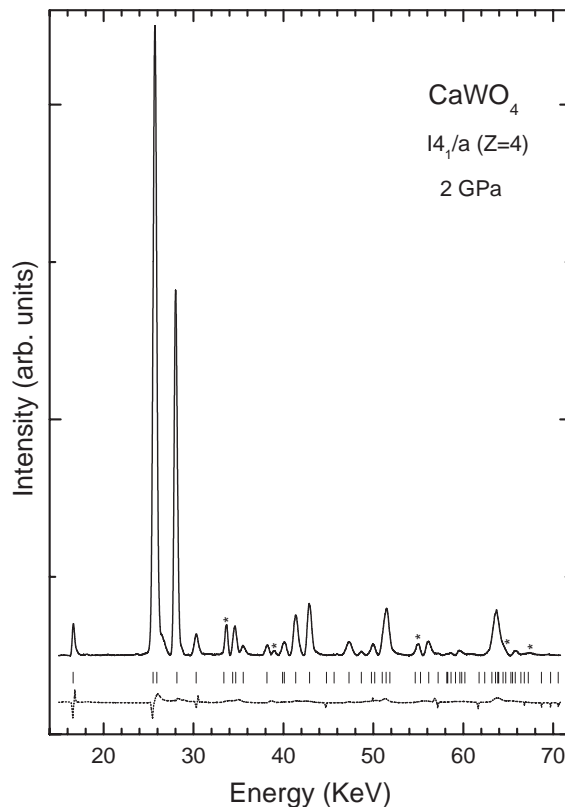


Fig. 2. EDXD pattern of the scheelite phase of  $CaWO_4$  at 2 GPa. The background was subtracted. The stars mark the position of the diffraction lines of the Au pressure marker. The last line represents the difference between the measured data and the refined profile. The bars indicate the calculated positions of the  $CaWO_4$  reflections.

$\text{CaWO}_4$  were calculated after performing the structural refinements using the POWDERCELL programme package [17]. The analogous data on  $\text{YLiF}_4$ , used for the comparative analysis of the pressure effects on the scheelite compounds  $\text{CaWO}_4$  and  $\text{YLiF}_4$ , were obtained from Ref. [5]. This recent work reported the data obtained from angle-dispersive powder diffraction experiments performed at the ID9 beamline at the European Synchrotron Radiation Facility using a monochromatic beam ( $\lambda = 0.4203 \text{ \AA}$ ) and a DAC with methanol–ethanol as the pressure medium.

### 3. Results and discussion

#### 3.1. Pressure effects on the local atomic structure

In order to know the microscopic mechanisms governing the scheelite-to-monoclinic phase transitions in  $\text{CaWO}_4$  and  $\text{YLiF}_4$ , we analyzed the pressure dependence of the lattice parameters and bond distances in these two compounds. Fig. 3 shows the pressure dependence of the lattice parameters for the scheelite phase of  $\text{CaWO}_4$  and  $\text{YLiF}_4$ . Both these compounds show a clearly anisotropic character, the compressibility of the  $c$ -axis being larger in  $\text{CaWO}_4$ , and the compressibility of the  $a$ -axis being larger in  $\text{YLiF}_4$ . This behavior is reflected in Fig. 4, which shows that the  $c/a$  ratio in both the compounds evolves in a different way under pressure,  $c$  being more compressible than  $a$  in  $\text{CaWO}_4$  while the contrary is true for  $\text{YLiF}_4$ . The  $c/a$  axial ratio

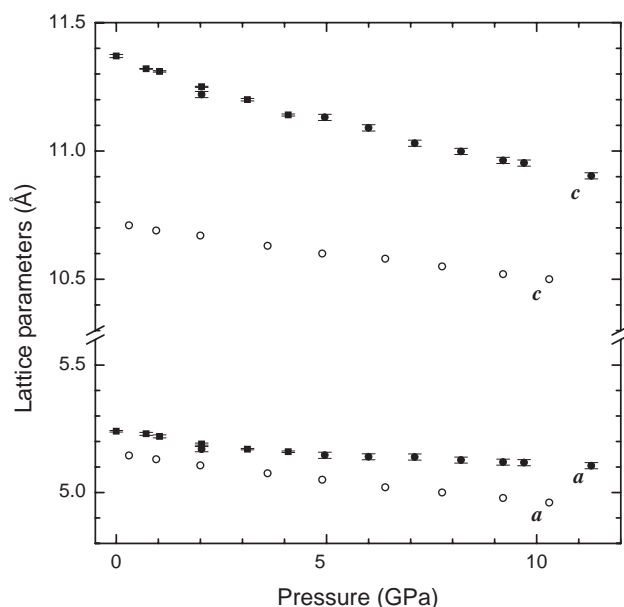


Fig. 3. Pressure dependence of the unit cell parameters of the scheelite structure in  $\text{CaWO}_4$  and  $\text{YLiF}_4$ . Data for  $\text{YLiF}_4$  (○) are taken from Ref. [5] and data for  $\text{CaWO}_4$  are from the present study (●) and Ref. [8] (■).

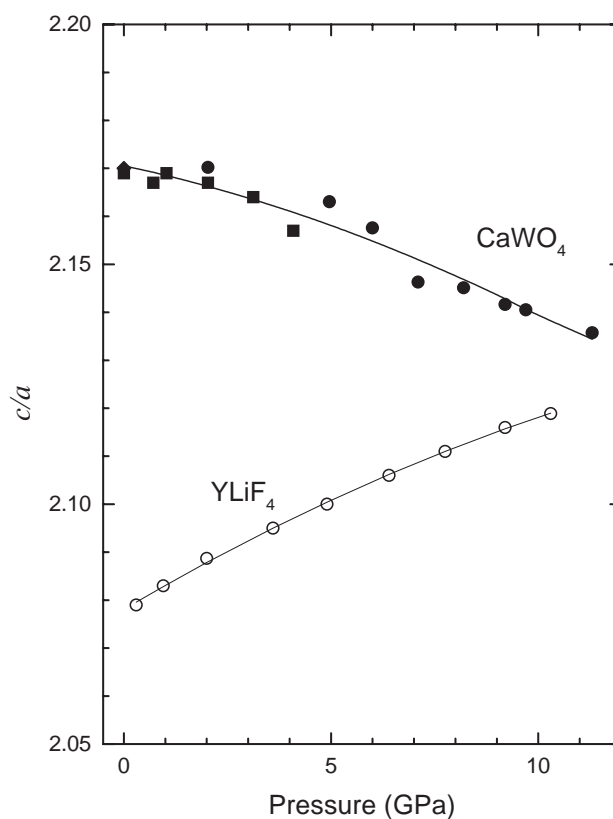


Fig. 4. Pressure dependence of the  $c/a$  ratio of the scheelite structure in  $\text{CaWO}_4$  and  $\text{YLiF}_4$ . Data for  $\text{YLiF}_4$  (○) are taken from Ref. [5] and data for  $\text{CaWO}_4$  are from the present study (●), Ref. [7] (◆), and Ref. [8] (■). The lines are just a guide for the eye.

decreases under compression from 2.17 at ambient conditions (1 bar) [8] to 2.136 at 11.3 GPa in  $\text{CaWO}_4$  [3], but it increases from 2.08 at 1 bar to 2.12 at 11 GPa in  $\text{YLiF}_4$  [5]. This difference in the behavior of the  $c/a$  ratio under pressure in  $\text{CaWO}_4$  and  $\text{YLiF}_4$  was previously noted by the different linear compressibilities of the lattice parameters measured in these two compounds [18].

In order to better understand the different anisotropic behavior of both the scheelites under pressure, it is very useful to describe them in terms of the pressure response of the  $AX_8$  and  $BX_4$  polyhedra. With this aim, the pressure dependence of the W–O distances inside the  $BX_4$  tetrahedra and the Ca–O distances inside  $AX_8$  polyhedra are plotted for  $\text{CaWO}_4$  in Fig. 5. The small pressure dependence of the W–O distance, as compared to that of the Li–F distance (see Fig. 4 in Ref. [5]), indicates that  $\text{WO}_4$  tetrahedra are rigid and isolated structural elements that undergo little change with pressure up to 11 GPa, unlike  $\text{LiF}_4$  tetrahedra, which are more compressible in the same pressure range. On the other hand, Ca–O (Y–F) bond compression is significantly greater (smaller) than that of the W–O (Li–F) bonds. These differences in the compressibilities

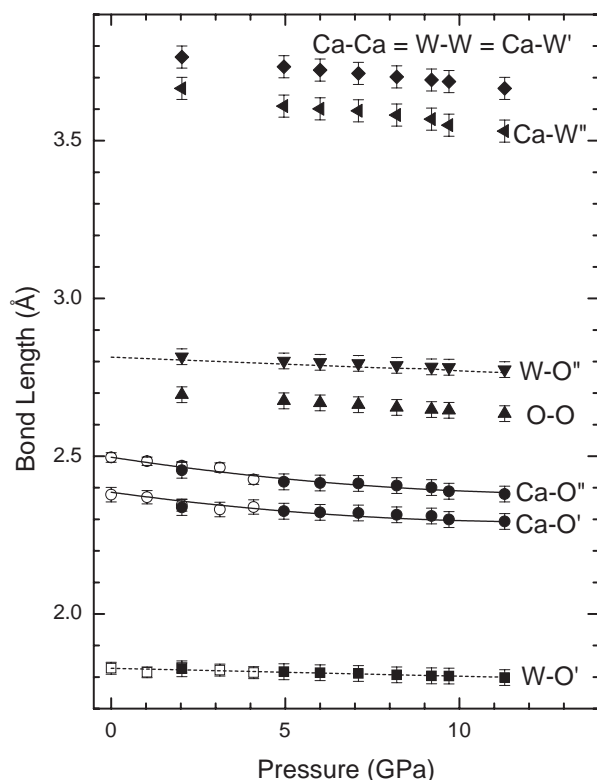


Fig. 5. Pressure dependence of the interatomic bonds in the scheelite structure of  $\text{CaWO}_4$ . The solid lines show the pressure dependence of the Ca–O bonds and the dashed lines the pressure dependence of the W–O bonds. The solid symbols are from the present study and the empty symbols from Ref. [8].

are the cause of the decrease (increase) of the  $c/a$  axial ratio in  $\text{CaWO}_4$  ( $\text{YLiF}_4$ ).

It is well known that the application of pressure reduces the interatomic distances and the atomic sizes, the large anions being more compressible than the small cations [19,20]. Therefore, the effect of pressure is twofold:

- (i) with increasing pressure the decrease of the interatomic distances and of cation sizes leads to an increase of the cation–cation repulsive forces [7, 21]; and
- (ii) the reduction of anion sizes leads to an increase of the packing efficiency of anions in the cationic sublattice.

According to Sleight [7], the increase of the cation–cation repulsion forces leads to a decrease of the  $c/a$  ratio tending to 2 in the tetragonal  $ABX_4$  compounds. This  $c/a$  value corresponds to that of the ideal structure for equal near-neighbor cation–cation distances and consequently to equal cation coordination. On the other hand, the increase of the anion packing efficiency leads to an increase of the  $c/a$  ratio and consequently to different cation coordination numbers.

Based upon these considerations, we think that the effect of pressure on the phase transitions depends greatly on which of the above two mechanisms predominate with the increase of pressure: cation–cation repulsion or anion packing efficiency. In this sense, it must be noted that the axial ratio of the scheelite structure of  $\text{YLiF}_4$  at atmospheric pressure is closer to  $c/a = 2$  than that of  $\text{CaWO}_4$ . Moreover, with increasing pressure this latter compound tends to the ideal structure for equal cation coordination while the former separates from it. On this basis, it can be concluded that the high-pressure phase transition of scheelites and the cation coordination of the high-pressure phase could be deduced with the help of the pressure dependence of the  $c/a$  ratio. At room pressure, in  $\text{CaWO}_4$  and  $\text{YLiF}_4$  the cation coordination is [8–4]. The decrease of the  $c/a$  ratio in  $\text{CaWO}_4$  with increasing pressure leads to a structure with cation coordination [6–6], as it is indeed in the wolframite structure. On the contrary, the increase of the  $c/a$  ratio in  $\text{YLiF}_4$  with increasing pressure leads to a structure with different cation coordination, as it occurs in M-fergusonite with a cation coordination between [8–4] and [8–6]. It is interesting to note that a similar increase of the  $c/a$  ratio with increasing pressure has been recently calculated in the ionic perrhenates  $\text{AgReO}_4$  and  $\text{NaReO}_4$  [22]. The scheelite perrhenates usually transform at high pressures to an orthorhombic pseudoscheelite structure, whose cation coordination is similar to that of the scheelite and M-fergusonite structures.

The experimental results agree with these previous considerations since the  $c/a$  ratio is larger for  $\text{CaWO}_4$  than for  $\text{YLiF}_4$ . This indicates that the  $\text{WO}_4$  group is more covalent than the  $\text{LiF}_4$  group, as it is indeed. As a consequence of this difference in covalence, there are smaller cation–cation repulsion forces in  $\text{CaWO}_4$  than in  $\text{YLiF}_4$  at atmospheric pressure. However, with increasing pressure cation–cation repulsion forces become dominant in  $\text{CaWO}_4$  while packing considerations become dominant in  $\text{YLiF}_4$  due to the increase in the covalence of the Y–F and Li–F bonds with increasing pressure. The decrease of the axial ratio in  $\text{CaWO}_4$  upon compression, especially above 5 GPa, could be related to just a small increase of the cation–cation electrostatic repulsion, which can be tentatively ascribed to a change in the electronic density around the Ca and W atoms. Furthermore, the change of cation coordination at the scheelite-to-wolframite transition could originate due to an  $s-d$  charge transfer effect [3]:

- (i) at low pressure, the occupation of the  $s$  orbital is favored [23], resulting in a more symmetrical distribution; and
- (ii) at high pressures, the occupation of a localized  $d$  orbital might induce a strong distortion, which would favor the transition to the wolframite

structure as it occurs in the temperature-driven tetragonal-to-monoclinic transition of  $\text{BiVO}_4$  [24].

On the other hand, the increase of the axial ratio in  $\text{YLiF}_4$  has been previously ascribed to the big ionic character of the fluorine bonds as compared to those formed by oxygen, the Y–F bond being less ionic and considerably less compressible than the Li–F bond. Therefore, the increase of the tetragonal distortion with increasing pressure was understood due to the big initial compressibility of the Li–F bond. The saturation in the increase of the axial ratio in  $\text{YLiF}_4$  above 6 GPa could be related to the stiffening of the Li–F bond, (see Fig. 4 in Ref. [5]), which would lead to a small increase of the cation–cation repulsion at the Li sites with increasing pressure due to the small size of the Li atoms.

Another interesting fact is that the reconstructive scheelite-to-wolframite transition in  $\text{CaWO}_4$  occurs together with a collapse of both the W–O bonds ( $1.798 \text{ \AA} \rightarrow 1.698 \text{ \AA}$ ) and the Ca–O bonds ( $2.293 \text{ \AA} \rightarrow 2.183 \text{ \AA}$  and  $2.379 \text{ \AA} \rightarrow 2.272 \text{ \AA}$ ) at the phase transition [3]. The reduction observed in the Ca–O distance is coherent with the occurrence of a change of the Ca ionic radii from  $1.12 \text{ \AA}$  (when Ca to O coordination is 8 in the scheelite phase) to  $1 \text{ \AA}$  (when Ca to O coordination is 6 in the wolframite phase) whereas the reduction of the W–O distances could be related to a change in the character of the bond. On the other hand, the fact that both bonds collapse at the transition is reflected in the fact that the axial ratio remains nearly constant during the transition (the  $2c/a$  ratio of the high-pressure wolframite phase is equal to the  $c/a$  ratio of the scheelite phase before the transition [3]). In addition, the scheelite-to-wolframite transition produces a distortion of the planes perpendicular to  $c$ . Basically, the crystal is deformed along one direction, making  $b > a$ . This fact is likely related to a tilting of the W–O polyhedra that could easily explain the occurrence of the scheelite-to-wolframite transition.

### 3.2. Phase transition mechanisms

In order to understand the scheelite-to-wolframite and scheelite-to-fergusonite transitions we have to note that:

- (i) the ionic–covalent bonds in the  $\text{ABX}_4$  fluorides are much weaker than the more covalent bonds in  $\text{ABX}_4$  oxides;
- (ii) long bonds are usually softer and more compressible than short ones;
- (iii) under compression almost all bonds become shorter (and most of them stronger); and
- (iv) upon the application of pressure cation–cation repulsive interaction increases considerably.

On this basis, it is commonly accepted that the atomic structures of  $\text{ABX}_4$  compounds under high pressures should tend to structures with a higher and equal coordination of both  $A$  and  $B$  cations [20]. The structural phase transitions shown by  $\text{CaWO}_4$  and  $\text{YLiF}_4$  point towards this direction because both the high-pressure monoclinic phases (wolframite and M-fergusonite) show larger average cation coordination than the scheelite structure [8–4]. In the wolframite structure, each  $A$  and  $B$  cation is in an approximately octahedral coordination surrounded by six near  $X$  sites [3,7]; i.e., with cation coordination [6–6], as shown in Fig. 6(a). A view of the cations in the wolframite structure is shown in Fig. 6(b). The [6–6] coordination in the wolframite phase suggests similar strengths for the forces associated to the W–O and Ca–O bonds in such a structure. In addition, this fact also points towards an increase of the coordination number around W cations with increasing pressure in the scheelite phase of  $\text{CaWO}_4$ . On the other hand, in the M-fergusonite structure, each  $A$  cation is surrounded by eight  $X$  anions and each  $B$  cation is surrounded by four  $X$  sites and two additional near  $X$  sites. Therefore, the M-fergusonite structure is considered as a deformed scheelite structure, which can be described as an intermediate structure between [8–4] and [8–6] cation coordination. Fig. 7 shows two views of the cation arrangement in the M-fergusonite structure.

The mechanism of the scheelite-to-wolframite transition in  $\text{CaWO}_4$  around 11 GPa is of a reconstructive nature and involves the destruction of both the diamond-like structures of Ca and W cations of the scheelite structure at the transition pressure. This reconstructive transition is due to the similar cation–cation repulsion forces at the Ca and W sites at a transition pressure that corresponds to similar Ca–O and W–O forces at the phase transition pressure. The similarity of Ca–O and W–O forces at the transition pressure is noteworthy despite the ionic and the covalent characters of the Ca–O and W–O bonds at ambient pressure, respectively [25]. From a short-range point of view, this phase transition mechanism is related to a shift of the W cation from the center of the  $\text{WO}_4$  tetrahedron towards the center of the  $\text{WO}_6$  octahedron, and it is characterized by

- (i) a motion of the W atoms from the center of the W–O tetrahedra along the  $b$  direction; and
- (ii) a shear displacement of its second neighbor O atoms.

Fig. 8(a) shows a schematic representation of the scheelite-to-wolframite transformation mechanism proposed here. Fig 8(b) shows the (100) projection of a section of the scheelite structure compared with that of a portion of the wolframite structure in order to better

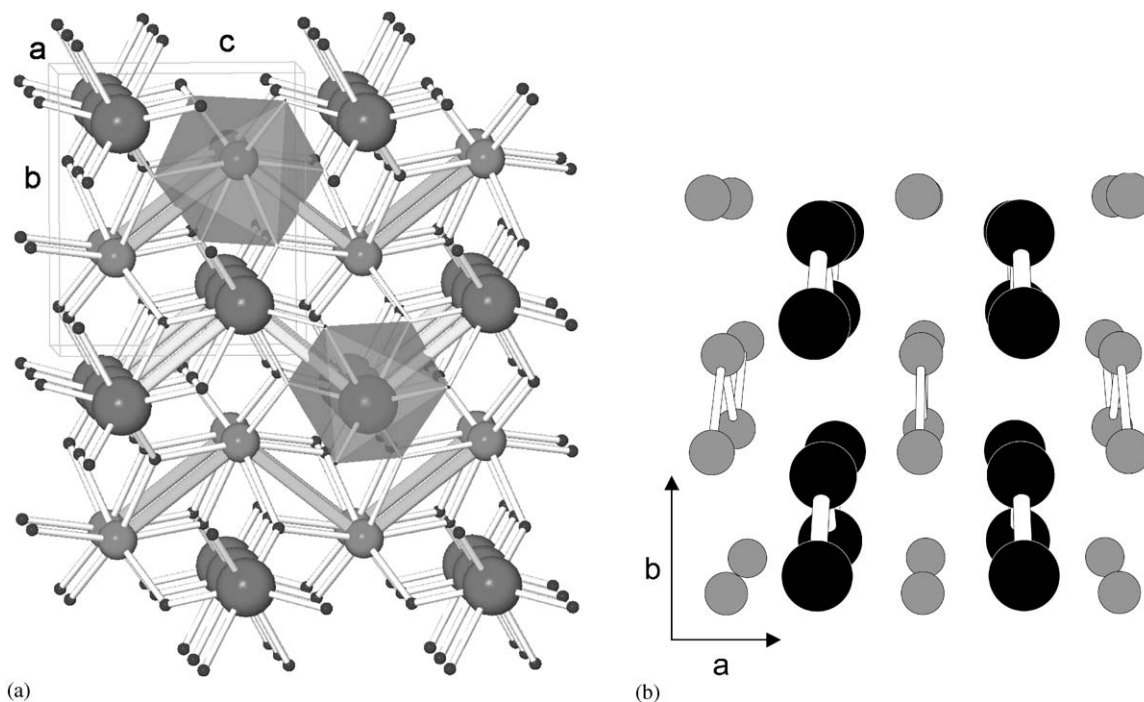


Fig. 6. (a) Wolframite structure of  $\text{CaWO}_4$  with its unit cell and the  $a$ -,  $b$ - and  $c$ -axis. (b) Wolframite structure of  $\text{CaWO}_4$  in the  $a$ - $b$  plane. The big black atoms refer to  $A$  cation (Ca), the gray medium-sized atoms correspond to  $B$  cation (W) and the small atoms to the  $X$  anion (O). The  $AX_6$  octahedra, the  $BX_6$  octahedra, and the shorter zig-zag cation–cation distances are also shown in (a) while anion atoms are not shown for the sake of clarity in (b). The shorter metal–metal distances are also shown in both schemes.

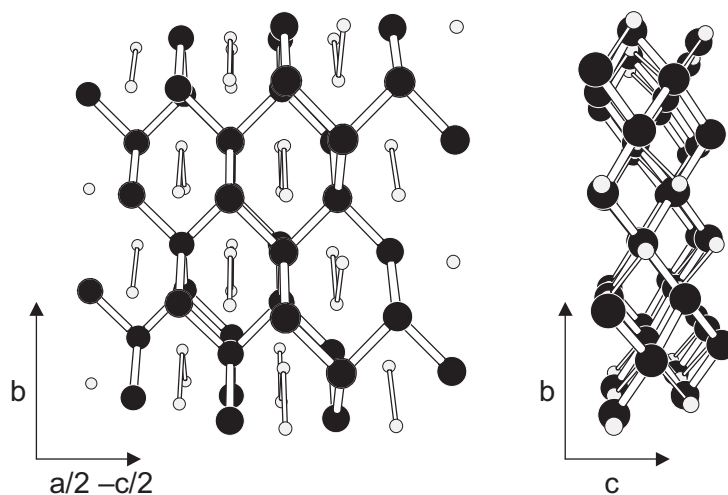


Fig. 7. Schematic views of the cationic arrangement in the M-fergusonite structure. The black atoms correspond to the  $A$  cation (Y), the gray atoms correspond to the  $B$  cation (Li). The anion atoms (F) are not shown for the sake of clarity. The shorter metal–metal distances are also shown.

illustrate the transformation. We believe that the process leading to the scheelite-to-wolframite transition is the following: at low pressure, the weak Ca–O bonding of the  $\text{CaO}_8$  polyhedra absorb much of the pressure while the  $\text{WO}_4$  tetrahedra remain as rigid units. When reaching around 10 GPa, the Ca–O bond length has decreased much more than the W–O bond length so as to become as strong as the W–O bond (see Fig. 5). Upon

further application of pressure, the W–O tetrahedral units are tilted and distorted and the [010] planes shear forming a distorted “Star of David” (see Fig. 8(b)). This configuration is characteristic of a cation in an octahedral coordination when viewed perpendicular to the  $c$ -axis of the scheelite (with four O atoms at 1.698 Å from W and two O atoms at 1.898 Å from W in the distorted octahedron).

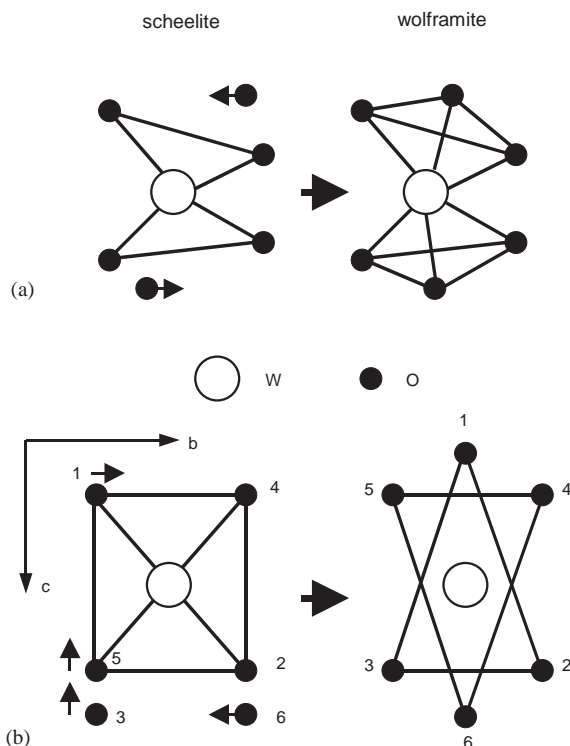


Fig. 8. (a) Schematic representation of the scheelite-to-wolframite model transition mechanism. (b) The (100) projection of a section of the scheelite structure compared to that of a portion of the wolframite structure. 1, 2, and 3 represent oxygen at  $(1/4, 0, 0)$  and 4, 5, and 6 oxygen at  $(-1/4, 0, 0)$ .

On the other hand, the mechanism of the scheelite-to-M-fergusonite transition in  $\text{YLiF}_4$  around 11 GPa is of a martensitic nature and it is preceded by a reversible polytype phase transition at 6 GPa. The  $\text{LiF}_4$  tetrahedra in the scheelite structure of  $\text{YLiF}_4$  form an angle  $\phi = 29^\circ$  with respect to the main  $a$ -axis at ambient pressure [18]. With increasing pressure, the Li–F distance decreases till the  $\text{LiF}_4$  tetrahedra become rigid around 6 GPa. At higher pressures, the stiffening of the Li–F bond (see Fig. 4 in Ref. [5]) and the progressive decrease of the  $a$  lattice parameter above 6 GPa is possible only if there is a gradual rotation of the  $\text{LiF}_4$  tetrahedra around the tetragonal  $c$ -axis; i.e., in the  $a$ – $b$  plane, toward larger angles. This fact means that the  $\text{LiF}_4$  tetrahedra can only rotate till they reach a maximum value of  $\phi = 45^\circ$  that is compatible with the scheelite structure and the reduction of the  $a$  lattice parameter. This rotation can be considered as a reversible phase transition from a polytype-I to a polytype-II scheelite structure. Polytype I is characterized by a setting angle  $\phi = 29^\circ$ , closer to the higher-symmetry zircon structure with  $\phi = 0^\circ$ , while polytype II is characterized by an angle  $\phi$  ( $29^\circ < \phi < 45^\circ$ ).

The reversible phase transition from scheelite polytype-I to polytype-II at 6 GPa in  $\text{YLiF}_4$  is induced by a polyhedral tilting (in this case rotation in the  $a$ – $b$

plane). This phase transition is possible due to the softening of one of the translational  $T(E_g)$  modes of the scheelite phase that involves a rotation of the  $\text{LiF}_4$  tetrahedra in the plane perpendicular to the  $c$ -axis [26]. It is worth noting that the softening of the  $T(E_g)$  mode of the zircon phase of  $\text{YVO}_4$  is also responsible for the zircon-to-scheelite phase transition above 7.5 GPa [27], since the  $\text{VO}_4$  tetrahedra in the zircon phase form an angle  $\phi = 0^\circ$  with respect to the main  $a$ -axis while that angle is always different from  $\phi = 0^\circ$  in the scheelite structure.

A characteristic of this kind of reversible transition is that the low-pressure structure (with higher symmetry) shows a certain degeneration of the vibrational modes, which disappears once the phase transition to the low-symmetry structure is accomplished [28]. A splitting of several Raman modes above 6 GPa that was initially overlapped is indeed observed [12,13]. Furthermore, this structural change around 6 GPa in  $\text{YLiF}_4$  is reflected in a slight modification of the pressure coefficients of the frequency of some  $\text{Nd}^{3+}$  crystal-field transitions above 6 GPa [6].

The reversible transitions show no major change in cation coordination, except for subtle displacements in the cation coordination of those cations with a larger coordination number. They also occur in a sudden and reversible manner leaving the crystal lattice undamaged during the transformation and with reduced volume changes. Furthermore, the reversible transitions are usually followed by twinning; i.e., a mixture of different lattice orientations of the new crystals due to the loss of a symmetry element in the phase transition. This fact can affect the accurate determination of the lattice parameters in the new structure and could be related to the strange behavior of the distances estimated in Ref. [5] from high-pressure X-ray diffraction measurements between 6 and 11 GPa. Moreover, the reversible phase transition around 6 GPa is coherent with the martensitic phase transition occurring at 10 GPa in  $\text{YLiF}_4$  since both reversible and martensitic transitions are common in ionic compounds [29,30]. As a matter of fact, they have also been found in other similar compounds like  $\text{KAlF}_4$  and  $\text{RbAlF}_4$  as a function of temperature and pressure [31,32].

Finally, the martensitic scheelite-to-M-fergusonite transition is a shear transformation in which the initial structure is partially conserved while certain sheets or pieces of the previous structure are slightly shifted. In  $\text{YLiF}_4$ , it involves a shift of the B (Li) cation long zigzag chains either along [100] or along [010] directions of the scheelite structure (see the schematic model shown in Fig. 9). Previous studies suggest that layer shifts along the [100] direction are energetically more favorable than shifts along [010] direction [33]. The large shift of B cations in  $\text{YLiF}_4$ , in contrast to what is observed in  $\text{CaWO}_4$ , is mainly due to the ionic character of the Li–F

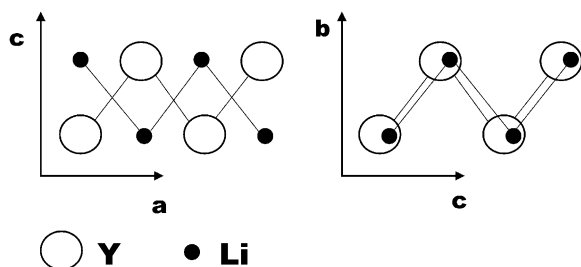


Fig. 9. Details of the scheelite structure (left) in the  $a$ – $c$  plane with A (Y) and B (Li) cations located in alternate planes along the  $b$ -axis (perpendicular to the paper). Details of the M-fergusonite structure (right) in the  $c$ – $b$  plane with A and B cations located in alternate planes along  $a$ -axis (perpendicular to the paper). The M-fergusonite structure derives from the scheelite structure when B cations shift along  $a$ -axis of the scheelite.

bond, which is much weaker than the covalent W–O in  $\text{CaWO}_4$ . This fact makes the Li atoms less tightly bound than the W atoms in the scheelite structure. This type of transition is quick and in certain cases the crystal is undamaged despite the symmetry of the final structure being lower than that of the previous one. These transformations are usually reversible; i.e., the initial structure is recovered on the release of pressure, but they usually show a certain hysteresis; a behavior indeed found in the scheelite-to-M-fergusonite phase transition in  $\text{YLiF}_4$  above 10 GPa [6].

This scheelite-to-M-fergusonite phase transition takes place because cation–cation repulsion increases considerably above 10 GPa, especially at the Li sites, which leads to the destruction of the Li diamond-like structure at the transition pressure whereas the Y diamond-like structure is preserved and slightly distorted. The well-known M-fergusonite structure is related to the scheelite structure, since it can be considered as a distorted scheelite (see the comparison view of both structures in Fig. 9), and conversely the scheelite structure can be viewed as a tetragonal fergusonite [30]. The larger increase of the repulsion at the Li sites as compared to the Y sites is likely due to a major change in the electronic density around the Y atoms with increasing pressure. This change in the electronic density around the Y atoms occurs because of the  $s$ – $d$  charge transfer previously commented [34] and does not affect the Li atoms. The slight distortion of the Y diamond-like lattice and the shift of the Li cations allow us to understand the martensitic second-order phase transition nature of the scheelite-to-M-fergusonite transition that proceeds without the volume change, as demonstrated by Gingerich and Bair [35].

Several additional facts support the above-described mechanisms for the scheelite-to-monoclinic phase transitions in  $\text{CaWO}_4$  and  $\text{YLiF}_4$ . There is a vision that the oxide scheelites can be considered as having a complex

layer-like structure, the layers being perpendicular to the  $c$ -axis and formed by a CsCl-type arrangement of A and  $\text{BO}_4$  ions [33]. This view of oxide scheelites as complex layer structures is supported by the large values of the  $c/a$  ratios of these compounds at ambient conditions, as compared to those of nearly ideal fluoride scheelites. Therefore, the decrease of the axial ratio in  $\text{CaWO}_4$  with increasing pressure tending to the ideal structure is in agreement with the tendency of several scheelite oxides to transform to the wolframite structure with increasing pressure [36]. In summary, oxide scheelites show a tendency towards a layer-like structure, unlike fluoride scheelites. In this sense, the high-pressure scheelite-to-wolframite transition is expected in  $\text{CaWO}_4$  because the wolframite structure also has a layer-like structure, unlike the M-fergusonite one. The layer-like structure of the wolframite structure along the  $a$  direction can be observed in Fig. 6(b).

The different tendencies of the oxide and fluoride scheelites towards the layer-like structure due to their different nature is also reflected in the thermal expansion coefficients of oxide and fluoride scheelites. In fluoride scheelites, the  $\alpha_{11}$  tensor component of the thermal expansion is greater than the  $\alpha_{33}$ , whereas in oxide scheelites the contrary is true, as it is usual in layer-like crystals [11,37]. Furthermore, we believe that the different high-pressure structures observed in both these compounds are related to the different nature of bonds in  $\text{CaWO}_4$  and  $\text{YLiF}_4$  and exhibit a link with the different behaviors of the axial compressibilities and the different soft modes observed in both these compounds. In this respect, Blanchfield et al. noted the instability of these two compounds under application of shear stresses, as deduced from the softening of several lateral modes [10,11]. However, the soft modes with larger softening are not the same in  $\text{CaWO}_4$  and  $\text{YLiF}_4$ , pointing out a significant difference between both the compounds. This result agrees with the recent results of ion rigid calculations in  $\text{YLiF}_4$  [38] and with recent Raman scattering measurements under pressure [9,12,13]. In  $\text{CaWO}_4$  a softening of one of the translational zone center  $T(B_g)$  modes as the pressure increases has been observed [9], while in  $\text{YLiF}_4$  the mode that softens under pressure is one of the translational zone center  $T(E_g)$  modes [13,38]. These two modes are interrelated because both can be considered as external modes of the  $BX_4$  tetrahedra and their frequencies are greatly affected by the substitution of the A cation [39]. These vibrational modes are low-frequency modes in both the compounds and are associated to translations of the  $BX_4$  tetrahedra. The  $B_g$  mode is associated to the vibration of the  $BX_4$  tetrahedra along the tetragonal axis of the scheelite, whereas the  $E_g$  mode is related to the vibration of the  $BX_4$  tetrahedra in the plane perpendicular to the tetragonal axis of the scheelite. We think that the softening of these modes is indicative of the

increase in the B–B distances observed in the scheelite-to-monoclinic phase transitions.

As a summary, we may conclude that the mechanisms that lead to the scheelite-to-wolframite transition are:

- (i) an increase of the B–B distance, due to the translation of the  $BX_4$  tetrahedra along the  $c$ -axis but maintaining the same mass center as in the scheelite structure; and
- (ii) a tilt of the  $BX_4$  tetrahedra with respect to the  $c$ -axis (see Fig. 8).

Both the increase of the B–B distance along the  $c$ -axis of the scheelite and the tilt of the  $BX_4$  tetrahedra can be associated to the softening of the  $B_g$  mode.

Correspondingly, the mechanisms that lead to the scheelite-to-M-fergusonite transition are:

- (i) a rotation of the  $BX_4$  tetrahedra around the  $c$ -axis of the scheelite;
- (ii) a slight distortion of the  $Y$  diamond-like structure; and
- (iii) a translation of the  $BX_4$  tetrahedra along the  $a$  (or  $b$ ) directions of the scheelite, leading to an increase in the B–B distance along the  $b+c$  (or  $a+c$ ) direction of the scheelite (see Figs. 1 and 9).

Both the rotation and the translation of the  $BX_4$  tetrahedra along the  $a$  or  $b$  direction can be associated to the softening of the  $E_g$  mode.

### 3.3. Size criterion

We have attempted to correlate the packing ratio of the anionic  $BX_4$  units around the  $A$  cations and the known phase transition pressures in the scheelite  $ABX_4$  compounds. Table 1 summarizes the available data on the pressure studies of 16 different scheelite  $ABX_4$  compounds. In Fig. 10, we have plotted the transition pressure vs. the  $BX_4/A$  radii ratio because this ratio is the sum of the  $X/A$  plus the  $B/A$  effective ionic ratios. To calculate the  $BX_4/A$  values (given in Table 1), the ionic radii of  $A$ ,  $B$ , and  $X$  atoms were taken from the literature [51–54]. As a result, we have observed that the phase transition pressure increases as the ratio between the ionic radii ( $BX_4/A$ ) increases. From these data, the following equation for the transition pressure ( $P_C$ ) as a function of the ( $BX_4/A$ ) radii ratio can be obtained as

$$P_C \text{ (GPa)} = (1 \pm 2) + (10.5 \pm 2) (BX_4/A - 1). \quad (1)$$

This relationship indicates that for  $BX_4/A < 1$  the scheelite structure is hardly stable even at ambient pressure. To understand the physics underlying Eq. (1), we have to remember that both the effective ionic radii decrease in cations and anions with increasing pressure, the radius decrease being larger for the larger anionic radii, as already commented [19,20]. Therefore, the  $B/A$  ratio is almost constant with increasing pressure while

Table 1

Phase transition pressures and  $BX_4/A$  ratios for some scheelite compounds

Compound	$BX_4/A$ ratio	$P_C$ (GPa)	Ref.
KIO <sub>4</sub>	1.39	6.5	[40]
RbIO <sub>4</sub>	1.25	5.3	[41]
AgReO <sub>4</sub>	1.9	13 ± 1	[21]
KReO <sub>4</sub>	1.45	7.5	[42]
RbReO <sub>4</sub>	1.30	1.6	[42]
CaWO <sub>4</sub>	1.89	11 ± 1	[3,4]
SrWO <sub>4</sub>	1.76	10.5 ± 2	[2,43,44]
EuWO <sub>4</sub>	1.76	8 ± 1	[45]
PbWO <sub>4</sub>	1.66	4.5	[46]
BaWO <sub>4</sub>	1.47	6.5 ± 0.3	[43]
CdMoO <sub>4</sub>	2.03	12	[47]
CaMoO <sub>4</sub>	1.88	8.2 ± 0.4	[9]
SrMoO <sub>4</sub>	1.74	12.5 ± 0.5	[48]
PbMoO <sub>4</sub>	1.64	6.5 ± 3	[46,49]
CaZnF <sub>4</sub>	1.97	10	[50]
YLiF <sub>4</sub>	2.11	11 ± 1	[5,6,13]

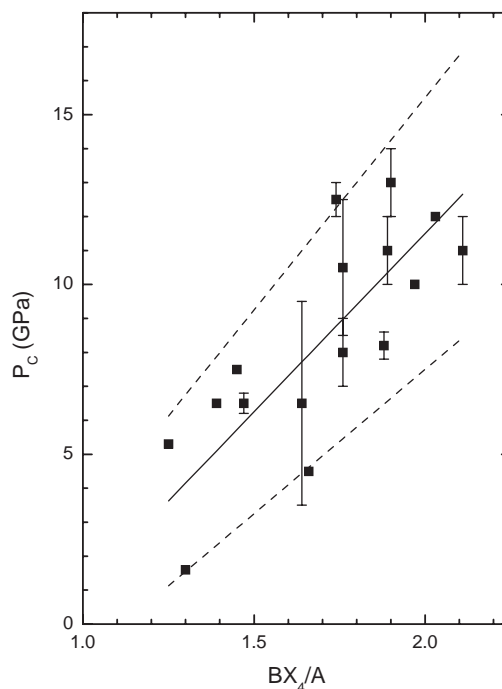


Fig. 10. Phase transition pressure in several scheelites as a function of the  $BX_4/A$  ratio. The symbols correspond to the data summarized in Table 1, the solid line corresponds to the relation given in Eq. (1), and the dashed lines indicate its lower and higher deviations.

the  $X/A$  ratio decreases considerably. Consequently, it is expected that the  $BX_4/A$  ratio decreases with increasing pressure and that those compounds showing a smaller  $BX_4/A$  ratio should exhibit lower transition pressures. This has already been empirically found in scheelite compounds, as shown in Table 1.

The above hypothesis for the instability of the scheelite compounds with  $BX_4/A$  radii ratios being near

or below 1 is also supported by the transition pressures found in the alkaline-earth perrhenates and periodates families [40–42,55]. It has been shown that  $\text{KReO}_4$ ,  $\text{RbReO}_4$ ,  $\text{KIO}_4$  and  $\text{RbIO}_4$  crystallize in the scheelite structure. However,  $\text{TlReO}_4$ ,  $\text{CsReO}_4$ , and  $\text{CsIO}_4$ , showing smaller  $BX_4/A$  ratios near 1, crystallize in a pseudoscheelite structure at ambient pressure, this structure being one of the high-pressure phases of perrhenates and periodates crystallizing in the scheelite structure at ambient pressure.

The above-given observations suggest that the proposed size criterion (which also effectively applies to  $A_2BX_4$  compounds [56]) could constitute a significant step towards unraveling the mechanisms underlying the pressure-driven transformations in scheelite compounds. Particularly, this simple criterion could be useful to predict the occurrence of pressure-driven instabilities in additional scheelite compounds like, e.g.,  $\text{ZrGeO}_4$ ,  $\text{NaReO}_4$ , and  $\text{KRuO}_4$ , for which Eq. (1) predicts the occurrence of pressure-driven phase transitions at 14.8, 11.5 and 7.3 GPa, respectively. Eq. (1) could also be helpful to estimate the pressure-driven instabilities in metastable scheelite compounds. Some of these compounds can be quenched at ambient pressure after a pressure cycle; as it occurs with  $\text{YVO}_4$  [57]. A phase transition near 11 GPa is estimated for this compound which could be related to the zircon to scheelite phase transition observed around 8 GPa.

As regards further high-pressure phase transitions in  $\text{CaWO}_4$  and  $\text{YLiF}_4$ , the wolframite structure of  $\text{CaWO}_4$  leads to an amorphous phase above 40 GPa [3]. However, the M-fergusonite structure of  $\text{YLiF}_4$  seems to lead to a new high-pressure phase still not determined above 17 GPa [5,13]. Several reports indicate that M- to M'-fergusonite phase transitions are common in ferroelastic materials under decrease of temperature or increase in pressure [58,59], the M' phase being isostructural to the baddeleyite structure (SG:  $P21/c$ , No. 14,  $Z = 2$ ) [1,2] or to the wolframite structure [59–61]. The M- to M'-fergusonite phase transition is of the reconstructive type with the unit cell of the baddeleyite structure similar to the wolframite unit cell. In this sense, the  $b$ -axis of the M-fergusonite is almost twice that of the wolframite or the baddeleyite, the  $a$ - and  $c$ -axis of the M-fergusonite being slightly smaller than those of the wolframite and the baddeleyite. Therefore, a phase transition to a baddeleyite (or wolframite) structure is likely expected for  $\text{YLiF}_4$  above 17 GPa. The transition to the baddeleyite structure would be consistent with the baddeleyite structure shown by  $\text{MnLiF}_4$  at ambient pressure, the  $\text{Mn}^{3+}$  ionic radius being smaller than that of  $\text{Y}^{3+}$ . Thus, the decrease of the Y ionic radius with increasing pressure could increase the instability of the M-fergusonite structure leading to the baddeleyite structure. On the other hand, the transition to the wolframite structure would also be possible and it

has been predicted by the recent electronic structure ab initio calculations performed using the VASP code [62]. New high-pressure X-ray diffraction studies of  $\text{YLiF}_4$  are required to answer definitively the new high-pressure structure.

#### 4. Concluding remarks

We report the pressure dependence of the lattice parameters and bond distances of the scheelite phase of  $\text{CaWO}_4$  and compare them to those previously reported for  $\text{YLiF}_4$ . The comparison of the thermal expansion coefficients and the pressure coefficients found for the lattice parameters, bond distances, and Raman modes in both the compounds has allowed us to understand why these two scheelites do not show the same high-pressure phase transitions. A mechanism for each of the two scheelite-to-monoclinic (wolframite or M-fergusonite) phase transitions has been proposed. Furthermore, from a comparative analysis of 16 different scheelite compounds, a close relationship between the phase transition pressures in scheelites and the  $BX_4/A$  radii ratio has been found. This simple criterion can be applicable to the search of new pressure-induced transformations in scheelite compounds.

#### Acknowledgments

The authors gratefully acknowledge the contribution of A. Vegas and A. Segura, who reviewed this paper and made valuable comments. They also thank Dr. J. Hu of beamline X-17C at NSLS for valuable technical advice and assistance. This work was supported by the NSF, the DOE, and the W.M. Keck Foundation. F.J.M. acknowledges financial support from the European Union under Contract No. HPMF-CT-1999-00074. D.E. also acknowledges the financial support from the MCYT of Spain through the “Ramón y Cajal” program for young scientists.

#### References

- [1] R.W.G. Wyckoff, *Crystal Structures*, Vol. 3, 2nd Edition, Wiley, New York, 1964, pp. 1–67.
- [2] T. Hahn (Ed.), *International Tables for Crystallography*, Vol. A, D. Riedel, Boston, 1987.
- [3] D. Errandonea, M. Somayazulu, D. Häusermann, *Phys. Stat. Sol. (b)* 235 (2003) 162.
- [4] D. Christofilos, S. Ves, G.A. Kourouklis, *Phys. Stat. Sol. (b)* 198 (1996) 539.
- [5] A. Grzechnik, K. Syassen, I. Loa, M. Hanfland, J.Y. Gesland, *Phys. Rev. B* 65 (2002) 104102.
- [6] F.J. Manjón, S. Jandl, K. Syassen, J.Y. Gesland, *Phys. Rev. B* 64 (2002) 235108.
- [7] A.W. Sleight, *Acta Crystallogr. B* 28 (1972) 2899.

- [8] R.M. Hazen, L.W. Finger, J.W.E. Mariathasan, *J. Phys. Chem. Solids* 46 (1985) 253.
- [9] D. Christofilos, G.A. Kourouklis, S. Ves, *J. Phys. Chem. Solids* 56 (1995) 1125.
- [10] P. Blanchfield, G.A. Saunders, T. Hailing, *J. Phys. C* 15 (1982) 2081.
- [11] P. Blanchfield, T. Hailing, A.J. Miller, G.A. Saunders, B. Chapman, *J. Phys. C* 20 (1983) 3851.
- [12] E. Sarantopoulou, Y.S. Raptis, E. Zouboulis, C. Raptis, *Phys. Rev.* 59 (1999) 4154.
- [13] Q.A. Wang, A. Bulou, J.Y. Gesland, *cond-mat/0210491*, 2002.
- [14] D. Errandonea, M. Somayazulu, D. Häusermann, *Phys. Stat. Sol. (b)* 231 (2002) R1.
- [15] A. LeBail, H. Duroy, J.L. Fourquet, *Mater. Res. Bull.* 23 (1988) 447.
- [16] A.C. Larson, R.B. Von Dreele, Los Alamos National Laboratory Report LAUR, 2000, pp. 86–748.
- [17] W. Kraus, G. Nolze, *J. Appl. Crystallogr.* 29 (1996) 301.
- [18] P. Blanchfield, G.A. Saunders, *J. Phys. C* 12 (1979) 4673.
- [19] O. Fukunaga, S. Yamaoka, *Phys. Chem. Miner.* 5 (1979) 167.
- [20] J.P. Bastide, *J. Solid State Chem.* 71 (1987) 115 and references therein.
- [21] J.W. Otto, J.K. Vassiliou, R.F. Porter, A.L. Ruoff, *Phys. Rev. B* 44 (1991) 9223.
- [22] J. Spitaler, C. Ambrosch-Draxel, E. Nachbaur, F. Belaj, H. Gomm, F. Netzer, *Phys. Rev. B* 67 (2003) 115127.
- [23] Y. Zhang, N.A. Holzwarth, R.T. Williams, *Phys. Rev. B* 57 (1998) 12738.
- [24] L.E. Depero, L. Sangaletti, *J. Solid State Chem.* 129 (1997) 82.
- [25] J.R. Smyth, S.D. Jacobsen, R.M. Hazen, *Rev. Miner.* 41 (2000) 157 and references therein.
- [26] S.P.S. Porto, J.F. Scott, *Phys. Rev.* 157 (1967) 716.
- [27] A. Jayaraman, G.A. Kourouklis, G.P. Epinosa, A.S. Cooper, L.G. Van Uiter, *J. Phys. Chem. Solids* 48 (1987) 755.
- [28] R.G.J. Strens, *Miner. Mag.* 36 (1967) 565.
- [29] R.M. Hazen, L.W. Finger, *Comparative Crystal Chemistry*, Wiley, New York, 1982.
- [30] O. Müller, R. Roy, *The Major Ternary Structural Families*, Springer, Berlin, 1974.
- [31] A. Bulou, A. Gibaud, M. Debieche, J. Nouet, B. Hennion, D. Petitgrand, *Phase Transitions* 14 (1989) 47.
- [32] Q.A. Wang, G. Ripault, A. Bulou, *Phase Transitions* 53 (1995) 1.
- [33] A. Arbel, R.J. Stokes, *J. Appl. Phys.* 36 (1965) 1460.
- [34] Y.K. Vohra, H. Olijnik, W. Grosshans, W.B. Holzapfel, *Phys. Rev. Lett.* 47 (1981) 1065.
- [35] K.A. Gingerich, H.E. Bair, *Adv. X-ray Anal.* 7 (1964) 22.
- [36] J. Macavei, H. Schulz, *Z. Kristallogr.* 207 (1993) 193.
- [37] V.T. Deshpande, S.V. Suryanarayana, R.R. Pawar, *Acta Crystallogr. A* 24 (1968) 398; V.T. Deshpande, S.V. Suryanarayana, *J. Phys. Chem. Solids* 30 (1969) 2484.
- [38] A. Sen, S.L. Chaplot, R. Mittal, *J. Phys.: Condens. Matter* 14 (2002) 975.
- [39] S. Salaün, M.T. Feroni, A. Bulou, M. Rousseau, P. Simon, J.Y. Gesland, *J. Phys.: Condens. Matter* 9 (1997) 6941.
- [40] T.A. Al Dhahir, H.L. Bhat, P.S. Narayanan, A. Jayaraman, *J. Raman Spectrosc.* 22 (1991) 567.
- [41] N. Chandrabhas, A.K. Sood, *Phys. Rev. B* 51 (1995) 8795.
- [42] A. Jayaraman, G.A. Kourouklis, L.G. Van Uiter, W.H. Grodkiewicz, R.G. Maines Sr., *Physica A* 156 (1988) 325.
- [43] A. Jayaraman, B. Batlogg, L.G. Van Uiter, *Phys. Rev. B* 28 (1983) 4774.
- [44] D. Christofilos, K. Papagelis, S. Ves, G.A. Kourouklis, C. Raptis, *J. Phys.: Condens. Matter* 14 (2002) 12641.
- [45] D. Errandonea, unpublished.
- [46] A. Jayaraman, B. Batlogg, L.G. Van Uiter, *Phys. Rev. B* 31 (1985) 5423.
- [47] S.R. Shieh, L.C. Ming, A. Jayaraman, *J. Phys. Chem. Solids* 57 (1996) 205.
- [48] A. Jayaraman, S.Y. Wang, S.R. Shieh, S.K. Sharma, L.C. Ming, *J. Raman Spectrosc.* 26 (1995) 451.
- [49] N. Ganguly, M. Nicol, *Phys. Stat. Sol. (b)* 79 (1977) 617.
- [50] Q.A. Wang, S. Salaün, A. Bulou, *cond-mat/0210553*, 2002.
- [51] R.D. Shannon, *Acta Crystallogr. A* 32 (1976) 751.
- [52] R.D. Shannon, C.T. Prewitt, *Acta Crystallogr. B* 25 (1969) 925.
- [53] R.D. Shannon, C.T. Prewitt, *Acta Crystallogr. B* 26 (1970) 1046.
- [54] J.E. Huheey, E.A. Keiter, R.L. Keiter, *Inorganic Chemistry: Principles of Structure and Reactivity*, 4th Edition, HarperCollins, New York, 1993.
- [55] N. Chandrabhas, D.V.S. Muthu, A.K. Sood, H.L. Bhat, A. Jayaraman, *J. Phys. Chem. Solids* 92 (1992) 959.
- [56] G. Serghiou, H.J. Reichmann, R. Boehler, *Phys. Rev. B* 55 (1997) 14765.
- [57] G. Chen, N.A. Stump, R.G. Haire, J.R. Peterson, M.M. Abraham, *Solid State Commun.* 84 (1992) 313.
- [58] G.A. Wolten, A.B. Chase, *Am. Miner.* 52 (1967) 1536.
- [59] Yu.A. Titov, A.M. Sych, A.N. Sokolov, A.A. Kapshuk, V.Ya. Markiv, N.M. Belyavina, *J. Alloys Compounds* 311 (2000) 252.
- [60] V.Ya. Markiv, N.M. Belyavina, M.V. Markiv, Yu.A. Titov, A.M. Sych, A.N. Sokolov, A.A. Kapshuk, M.S. Slobodyanyk, *J. Alloys Compounds* 346 (2002) 263.
- [61] G.A. Wolten, *Acta Crystallogr.* 23 (1967) 939.
- [62] S. Li, R. Ahuja, B. Johansson, in press.